

# Analysis of High Efficiency Multistage Matching Networks with Volume Constraint

Phyo Aung Kyaw, Aaron L.F. Stein, Charles R. Sullivan

Thayer School of Engineering at Dartmouth

Hanover, NH 03755, USA

{phyo.a.kyaw.th, aaron.l.stein, charles.r.sullivan}@dartmouth.edu

**Abstract**—Matching networks have useful applications in transforming voltages and impedances in resonant inverters and dc-dc converters. Stacking multiple stages of matching networks can, in some cases, increase the efficiency because each stage is responsible for smaller transformation, but it also reduces the available inductor volume for each stage which can increase the loss. We present optimization of matching networks with volume constraints to determine the optimum number of stages and other design choices for various transformation ratios, volumes and impedances. Scaling models of inductor performance with size are presented and their effect on the efficiency of single-stage and multistage matching networks is analyzed. The analytical results are verified by an experiment using 1- and 2-stage matching networks with a total volume constraint and a voltage transformation ratio of 4. Simple design rules for designing matching networks are presented for voltage transformation ratios lower than 20.

## I. INTRODUCTION

Matching networks, two-port circuits for impedance and voltage transformations, are widely used in RF communications. In power electronics, they have useful applications in resonant inverters and dc-dc converters, and analysis and design considerations for high efficiency matching networks are described in [1]. Assuming inductors with a fixed maximum quality factor (fixed-Q case), and purely resistive input and load impedances for each stage, that analysis derives an upper bound on the optimum number of stages that should be used for any desired voltage transformation ratio.

The assumption of a fixed quality factor means that adding an extra stage to a matching network also increases the volume. However, practical design scenarios usually limit the available volume. Thus, adding a total volume constraint to the analysis in [1] can provide insights into the optimum number of stages that need to be used in practical designs.

Relaxing the resistive impedance assumed in [1] gives a different design framework [2], and results in optimal efficiencies higher than those derived in fixed-Q resistive-impedance analysis in [1]. These implications are discussed further in Section IV-C. In this paper, however, we assume purely resistive input and load impedances for each stage, similar to the analysis in [1].

Inductor performance usually degrades as the volume gets smaller [3]–[6]. Thus, inductors required for a 2-stage matching network will individually have a lower quality factor than that for a single-stage matching network of the same total volume. To account for the decrease in inductor quality factor

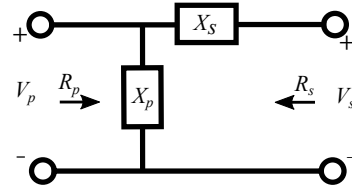


Fig. 1. An L-section matching network transforming a high shunt-leg voltage  $V_p$  to a low series-leg voltage  $V_s$ .

as the number of stages increases, we apply scaling laws for inductor quality factor with size. We then examine the effects of these scaling laws on the efficiency of matching networks with a total volume constraint (fixed-volume case).

Matching network design equations are presented in Section II. We present in Section III two inductor scaling models, namely scaling of linear dimensions [3] and optimizing inductor dimensions [7], that describe the degradation of inductor performance as it scales down in size. The scaling models are then combined with matching network design equations in Section IV to examine the trade-off between inductor quality factor and voltage transformation ratio in a multistage matching network. We also present simple design rules for choosing the number of stages, and the transformation ratio and volume of each stage. The effects of linear scaling of inductor dimensions on matching network efficiency are verified in Section V using 1- and 2-stage networks with a voltage transformation ratio of 4 in a total volume of 1 cm<sup>3</sup>.

## II. MATCHING NETWORK DESIGN EQUATIONS

We first present basic equations for designing matching networks [1]. We assume L-section networks (Fig. 1), which can be stacked together in a multistage configuration. Although equivalent T- and II-section networks with similar voltage transformation can be designed, they usually have lower efficiency than L-section networks [1].

For transformation from a high shunt-leg voltage  $V_p$  to a low series-leg voltage  $V_s$ , the transformation quality factor is

$$Q_t \equiv \sqrt{v_r^2 - 1}, \text{ where } v_r = \frac{V_p}{V_s}. \quad (1)$$

To achieve the desired transformation, the passive components need to be chosen such that  $Q_t$  equals both the shunt-leg quality factor  $Q_p = R_p/|X_p|$  and the series-leg quality factor  $Q_s = |X_s|/R_s$ .  $|X_p|$  and  $|X_s|$  are magnitudes of the reactances of the passive components used in the shunt-leg and

the series-leg respectively. The resistances  $R_p$  and  $R_s$  refer to the resistances looking into the two legs and are related to  $V_p$  and  $V_s$  by  $R_p/R_s = V_p^2/V_s^2$ ; they do not relate to the ESR of the required capacitors and inductors [1].

The efficiency of such an L-section matching network depends on the ESR, hence the quality factor, of the required passive components. The quality factor of an inductor is  $Q_L \equiv \omega L/R_L$  and that of a capacitor is  $Q_C \equiv 1/(\omega C R_C)$ , where  $R_L$  is the inductor ESR and  $R_C$  the capacitor ESR. Capacitors are in general much more efficient and have higher quality factors than inductors, and it is assumed in this paper that  $Q_C \gg Q_L$ . Thus, losses and volumes of the required capacitors are much smaller than those of the inductors and are ignored in the analysis. The efficiency is given by [1]

$$\eta \approx 1 - \frac{Q_t}{Q_L} - \frac{Q_t}{Q_C} \approx 1 - \frac{Q_t}{Q_L}. \quad (2)$$

The efficiency of an  $n$ -stage matching network is the product of the efficiency of each stage,

$$\eta = \prod_{i=1}^n \eta_i \approx \prod_{i=1}^n \left( 1 - \frac{Q_{ti}}{Q_{Li}} \right), \quad (3)$$

where  $Q_{ti}$  and  $Q_{Li}$  are respectively the transformation quality factor and the inductor quality factor of the  $i$ -th stage.

Each stage of a multistage matching network is responsible for a smaller voltage transformation ratio and so has a smaller  $Q_{ti}$  than does a single-stage network. On the other hand, the available volume for each inductor in a multistage network is smaller than that in a single-stage network, resulting in a lower  $Q_{Li}$ . Thus, a multistage matching network may be favorable compared to a single-stage network of the same volume depending on how the inductor quality factor scales with volume, which we investigate in the following section.

### III. INDUCTOR SCALING

The quality factor  $Q_L$  of an inductor can be calculated as  $\omega L/R_L$  where  $\omega$  is the angular frequency,  $L$  the inductance and  $R_L$  the inductor ESR. Assuming a base quality factor  $Q_{L0}$  for an inductor of base volume  $\mathcal{V}_{L0}$ , the quality factor  $Q_L$  of an inductor in a different volume  $\mathcal{V}$  can be calculated using some scaling models. We use two different scaling models, namely linear scaling of all dimensions and optimizing the inductor design for various volumes, assuming air-core inductors limited by the skin-depth. Scaling of linear dimensions is used in [3] to examine the loss and VA capability of inductors under various constraints; the same scaling concept is used here and the analysis is extended to include the inductance and the quality factor of inductors. Optimization of the inductor design based on inductor ESR and frequency is presented in [7], and that analysis is extended here to include the effect of inductance and available volume on the inductor quality factor.

#### A. Simple scaling of linear dimensions

The inductance of any inductors can be expressed as

$$L = N^2 \mu \frac{A_m}{l_m}, \quad (4)$$

where  $N$  is the number of turns in the winding,  $\mu$  the permeability,  $A_m$  the effective magnetic flux area and  $l_m$  the effective magnetic path length. If all the linear dimensions are scaled by a factor  $\epsilon$ , the area  $A_m$  scales as  $\epsilon^2$  and the length  $l_m$  scales as  $\epsilon$ , resulting in  $L \propto \epsilon$ . The skin-effect limited inductor ESR is given by

$$R_L = N^2 \rho \frac{l_w}{b_w \delta}, \quad (5)$$

where  $l_w$  is the length of conductor loop in the winding,  $b_w$  the winding breadth and  $\delta$  the skin-depth. Because  $\delta$  only depends on the frequency and conductor material properties,  $R_L$  is independent of  $\epsilon$ , resulting in  $Q_L = \omega L/R_L \propto \epsilon$ .

Simply scaling all the linear dimensions without changing the number of turns  $N$  changes both  $L$  and  $Q_L$ . Because the required  $L$  depends on the desired voltage transformation ratio  $v_r$ , the dependence of  $Q_L$  on  $L$  also affects the matching network efficiency. However, for large enough inductance which requires many turns of wire, the number of turns  $N$  gives an independent variable to approximately obtain the desired  $L$ . Changing  $N$  does not affect  $Q_L$  because both  $L$  and  $R_L$  are proportional to  $N^2$ . Thus, it can be concluded that

$$Q_L \propto L^0 \epsilon \propto L^0 \mathcal{V}_L^{1/3}, \quad (6)$$

where the second proportionality results from  $\mathcal{V}_L \propto \epsilon^3$ . This is strictly correct only when all dimensions are scaled by the same factor. However, as will be discussed in Section III-B,  $Q_L \propto \mathcal{V}_L^{1/3}$  even if the three dimensions of the inductor are not scaled by the same factor. We include  $L$  raised to the zeroth power in (6) to emphasize that the quality factor is independent of  $L$ .

Let's examine the case of halving all the linear dimensions of a base inductor with a volume  $\mathcal{V}_{L0}$ , inductance  $L_0$ , ESR  $R_{L0}$  and quality factor  $Q_{L0}$ . The resulting inductor, with the same number of turns as the base inductor, will have a volume  $\mathcal{V} = \mathcal{V}_0/8$ , with inductance  $L = L_0/2$ , ESR  $R_L = R_{L0}$  and quality factor  $Q_L = Q_{L0}/2$ . If a different inductance value is desired, it can be obtained by changing the number of turns  $N$  without changing  $Q_L$ .

The scaling of linear dimensions provides a simple way to calculate the quality factor of an inductor of any size using the quality factor and the size of an optimally designed base-case inductor. However, simply scaling all the linear dimensions does not guarantee that the resulting inductor will have an optimum design, and inductors usually have to be custom designed for the available space and particular applications [3]. Moreover, linear scaling of all dimensions and the resulting proportionality are only approximate because the number of turns can only be an integer and wires are only readily available in some standard sizes. In addition, because inductors with fewer than one turn are physically impossible, there is a lower limit on the inductance achievable without impacting the quality factor. Thus, if a very low inductance is required, the model of scaling linear dimensions breaks down and a single-turn inductor needs to be designed with specific dimensions.

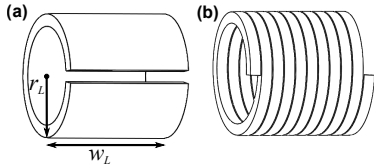


Fig. 2. Single-layer solenoids with rectangular conductor; (a) single-turn, (b) multi-turn.

### B. Optimizing inductor design

Optimization of inductor design depends on the type of inductor. We assume an air-core solenoid in this paper; however, the results can also be applied to toroids and inductors with a magnetic core operated in the linear regime. The solenoid can be single-turn or multi-turn and is wound with a rectangular conductor (Fig. 2). The conductor thickness is assumed to equal the skin-depth  $\delta$  and the winding is limited to be a single-layer to minimize proximity effect losses at MHz frequencies.

Assuming that the skin-depth is much smaller than the inductor dimensions, we can derive the inductance, the inductor ESR and the quality factor as

$$L = \frac{N^2 \mu K \pi r_L^2}{w_L} = \frac{N^2 \mu K \pi^2 r_L^4}{\mathcal{V}_L}, \quad (7)$$

$$R_L \approx \frac{N^2 \rho 2\pi r_L}{w_L \delta} = \frac{N^2 \rho 2\pi^2 r_L^3}{\mathcal{V}_L \delta}, \quad (8)$$

$$Q_L \approx 2\pi f \mu K r_L \frac{\delta}{2\rho} = \frac{r_L K}{\delta}, \quad (9)$$

where  $r_L$  is the solenoid radius,  $w_L$  the solenoid width,  $K$  the Nagoka coefficient which is a correction factor for the end effects in an air-core coil of finite length [7], [8] and  $\mathcal{V}_L$  the inductor volume. The second equalities in (7) and (8) result from the volume constraint  $\mathcal{V}_L = \pi r_L^2 w_L$ .

If a large inductance is required for the desired voltage transformation, a solenoid with a multi-turn winding and/or a cross-section larger than the length is needed. However, because the reluctance of the flux path for such a short solenoid is dominated by the return path reluctance, using a larger number of turns is more efficient than using a larger radius [7]. Thus, the required  $L$  can be achieved by varying  $N$ ; this does not affect  $Q_L$  since both  $L$  and  $R_L$  are proportional to  $N^2$ . Thus, it can be concluded that  $Q_L \propto L^0 r_L \propto L^0 \mathcal{V}_L^{1/3}$ , the same result as in (6) for simple scaling of linear dimensions. The first proportionality is only approximate because (7) and (8) do not account for the thickness  $\delta$  of the conductor, which becomes significant as the volume gets smaller. Because  $Q_L$  depends on  $\delta$  (9), the constant of proportionality and  $Q_L$  vary with the square root of the frequency.

The proportionality  $Q_L \propto \mathcal{V}_L^{1/3}$  is derived from the proportionality  $Q_L \propto r_L$  or  $Q_L \propto \epsilon$  assuming that all dimensions are scaled by a scaling factor  $\epsilon$ , which results in  $\mathcal{V}_L \propto \epsilon^3$ . However,  $Q_L \propto \mathcal{V}_L^{1/3}$  can be considered approximately true even if all the dimensions are not scaled by the same factor. A specific inductance can be achieved inside a particular volume using various number of turns if the inductor aspect ratio is adjusted accordingly. For example, Fig. 3 shows the achievable

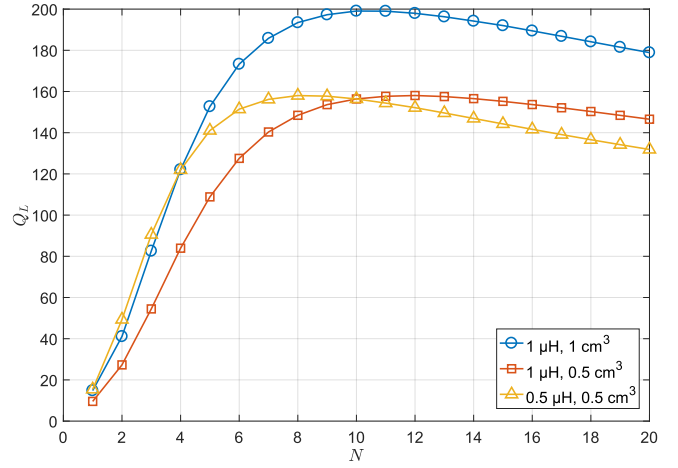


Fig. 3. The quality factor as a function of the number of turns for 1 cm<sup>3</sup> and 0.5 cm<sup>3</sup> inductors at 13.56 MHz. The inductance is the same along each curve, obtainable by varying the inductor aspect ratio. The peak values of  $Q_L$  for all three curves are obtained at the same aspect ratio.

quality factor of a 1 μH inductor within a 1 cm<sup>3</sup> volume at 13.56 MHz as a function of the number of turns in the winding; a quality factor as high as 200 can be achieved using 10 turns. However, the peak in the  $Q_L$  vs.  $N$  curve is broad enough that  $Q_L$  only decreases to 197 for  $N = 9$  and 196 for  $N = 13$ . This difference in  $N$  means that the aspect ratios of the 9-turn and 13-turn inductors are different in order to achieve the same inductance. However, both inductors have  $Q_L$  approximately equal to the optimal quality factor. Fig. 3 also shows the achievable quality factor for inductors with half the volume (0.5 cm<sup>3</sup>) and two different inductances. These half-volume inductors have a maximum quality factor of around 158 ( $\approx 200/\sqrt[3]{2}$ ), with the same broad peak. Thus,  $Q_L$  is reduced by approximately a factor of  $\sqrt[3]{2}$  if the volume is halved, with or without preserving the aspect ratio. Thus, it can be concluded that  $Q_L \propto \mathcal{V}_L^{1/3}$  even if all the inductor dimensions are not scaled by the same factor.

For small inductances,  $N$  is limited to unity and the solenoid needs to be thin and long, in which case  $K \approx 1$ . The dependence of  $Q_L$  on  $L$  can be derived from (7) and (9) as

$$r_L = \left( \frac{L \mathcal{V}_L}{N^2 \mu K \pi^2} \right)^{1/4} = \left( \frac{L \mathcal{V}_L}{\mu \pi^2} \right)^{1/4}, \quad (10)$$

$$Q_L = \frac{r_L K}{\delta} = \frac{r_L}{\delta} = \frac{1}{\sqrt{\pi} \delta} \left( \frac{L \mathcal{V}_L}{\mu} \right)^{1/4}. \quad (11)$$

Thus,  $Q_L \propto L^{1/4} \mathcal{V}_L^{1/4}$  for small inductance values.

This effect of optimizing the inductor design can be visualized by a contour plot of  $Q_L$  as a function of the required  $L$  and the available volume. Fig. 4 shows such a contour plot for 13.56 MHz. When the required inductance is high (in the multi-turn regime above the boundary in Fig. 4),  $Q_L$  is independent of  $L$  and approximately proportional to  $\mathcal{V}_L^{1/3}$ . In this case, the optimization of inductor design converges to the simple scaling of linear dimensions because the required  $L$  is large enough that it can be varied by changing the number of turns  $N$  without affecting  $Q_L$ . On the other hand, if the

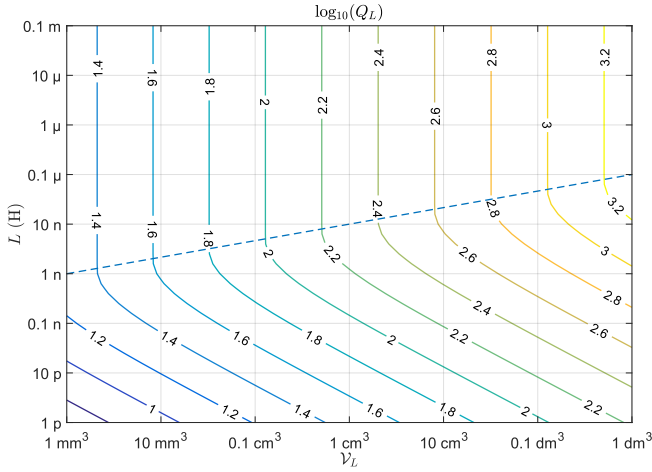


Fig. 4. Contour plot of log of the the maximum achievable inductor quality factor as a function of the required inductance and the available volume. The inductor winding is one skin-depth thick foil at 13.56 MHz. The blue dashed line represents an approximate boundary between the multi-turn inductor regime (vertical contours above the line) and the single-turn inductor regime (diagonal contours below the line).

required inductance is small (single-turn regime below the boundary in Fig. 4), a single-turn inductor is required and the quality factor converges to (11).

It should be noted that Fig. 4 is specific to 13.56 MHz and the single-layer solenoid (Fig. 2). However, the proportionalities in (6), (9) and (11), hence the shape of the contour plot, are applicable for different frequencies and non-magnetic-core toroids with a single-layer winding. The constants of proportionality will, however, be different depending on the operating frequency and the inductor geometry.

#### IV. MATCHING NETWORK OPTIMIZATION WITH A VOLUME CONSTRAINT

We have presented matching network design equations for calculating the required inductance and capacitance to achieve the desired transformation ratio and the efficiency of the resulting network. Depending on how the inductor performance varies with a constrained volume, it may be beneficial to increase the number of stages in a matching network. In this section, we present an analysis to determine when it is necessary to increase the number of stages to achieve the maximum possible efficiency. The scaling of inductor performance depends on the required inductance as discussed in Section III, which we use in this section together with matching network design equations to calculate the optimum number of stages for a matching network and the corresponding design choices.

##### A. Scaling of linear dimensions

The efficiency  $\eta$  of a matching network depends only on  $Q_t$  and  $Q_L$  as shown in (2) and is independent of  $L$  except for possible relations between  $L$  and  $Q_t$  or  $Q_L$ . The transformation quality factor  $Q_t$  depends on the desired transformation ratio  $v_r$  and the inductance  $L$  needs to be chosen such that  $Q_t$  equals the shunt-leg or the series-leg quality factor; thus, the value of  $L$  depends on  $Q_t$  and not vice versa. Moreover, the simple model of scaling linear dimensions in (6) results in  $Q_L$

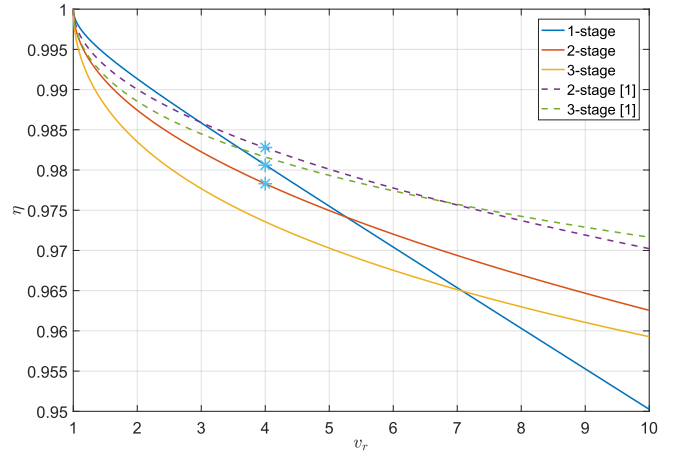


Fig. 5. Matching network efficiency  $\eta$  vs. voltage transformation ratio  $v_r$ , assuming the inductor quality for the base case is 200. Solid lines represents the fixed-volume analysis of this paper and dashed lines represent the fixed-Q case in [1]. The result for 1-stage matching network is the same for both cases. The 2-stage and 3-stage networks in the fixed-Q case respectively have double and triple the volume of the 1-stage network. The asterisks represent the operating point that will be verified experimentally in Section V.

that depends only on the volume  $\mathcal{V}_L$  and not on the required inductance  $L$  (Section III-A). Thus, in this case of scaling the linear dimensions, the matching network efficiency only depends on  $v_r$  and  $\mathcal{V}_L$ , and not on  $L$ .

For an  $n$ -stage matching network, the overall efficiency (2) needs to be maximized subject to the voltage transformation ratio constraint  $v_r = \prod_{i=1}^n v_{ri}$  and the volume constraint  $\mathcal{V} = \sum_{i=1}^n \mathcal{V}_i$ . Due to these constraints, it can be derived from (3) that the efficiency of a multi-stage network is maximum if the transformation ratio and the volume, hence the efficiency, of all the stages are equal. A similar result is derived in [1] for the fixed-Q case. Thus, for the maximum efficiency in an  $n$ -stage matching network, each stage should have a transformation ratio  $v_r^{1/n}$  and a volume  $\mathcal{V}/n$ .

Assuming that a base inductor quality factor  $Q_{L0} = 200$  is achievable within a base volume  $\mathcal{V}_{L0}$ , the efficiency of an  $n$ -stage matching network can be calculated for various  $v_r$ . For reference, this quality factor of 200 is theoretically achievable with a  $1 \text{ cm}^3$  volume at 13.56 MHz (Fig. 4). In a 2-stage network with  $v_r = 4$ , for example, each stage will have  $v_{ri} = 2$  with  $\mathcal{V}_i = \mathcal{V}_{L0}/2$ . This results in each inductor having  $Q_{Li} = Q_{L0}/\sqrt[3]{2} = 159$  and an overall matching network efficiency of  $(1 - \sqrt{2^2 - 1}/159)^2 \approx 0.978$ . This calculation is repeated for different  $v_r$  ranging from 1 to 100 and for various number of stages. Fig. 5 shows the efficiency of 1-, 2- and 3-stage matching networks with  $v_r$  ranging from 1 to 10. For comparison, the results of the fixed-Q analysis from [1] are also included in Fig. 5. Because of the smaller volume available for each stage in the fixed-volume case compared to the fixed-Q case of [1], the inductors have a lower quality factor, resulting in a lower efficiency for the fixed-volume case.

More important, the transformation ratio breakpoints above which it is more efficient to add an extra stage to the matching network are different for the two cases. For example, in the fixed-Q case of [1], a single-stage network is the most efficient

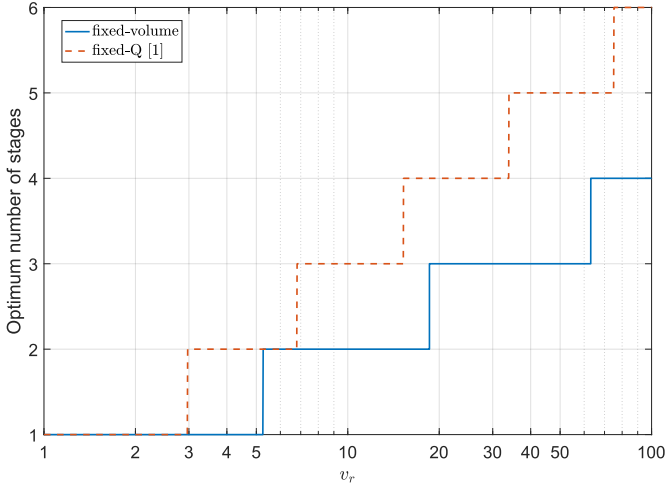


Fig. 6. Optimum number of stages vs. voltage transformation ratio  $v_r$ , calculated using  $Q_{L0} = 200$ .

for  $v_r \lesssim 3$  but in the fixed-volume case, the advantage of a single-stage network extends up to  $v_r \approx 5.3$ . Table I shows the optimum ranges of  $v_r$ , and the corresponding  $Q_L$  and total volume  $\mathcal{V}_{tot}$  for 1-, 2- and 3-stage networks for the fixed-volume analysis of this paper and the fixed-Q analysis of [1].

The optimum number of stages for various transformation ratios can be visualized as shown in Fig. 6. In the fixed-Q case, matching networks of up to 6 stages may be beneficial for  $v_r < 100$ . However, this is only an upper bound on the optimum number of stages since a more-efficient fewer-stage matching network may be designed using higher-Q inductors [1]. Constraining the design space by volume gives the optimum number of stages that should actually be used rather than an upper bound. This volume-constrained analysis shows that no more than 4 stages should be used for  $v_r < 100$ . An experimental verification for the difference between the two cases is discussed in Section V.

The results in Figs. 5 and 6 are calculated using a base quality factor  $Q_{L0} = 200$ , which approximately corresponds to the theoretical maximum quality factor of a  $1 \text{ cm}^3$  air-core solenoid with a single-layer winding (Fig. 2) at 13.56 MHz. The base quality factor will be different if the available volume or the operating frequency is different, or if practical implementation limits the achievable quality factor. In such cases, the efficiency curves in Fig. 5 will shift up or down depending on  $Q_{L0}$ . However, the optimum number of stages and the corresponding voltage transformation ratio breakpoints will remain approximately the same as those shown in Fig. 6.

### B. Design in the Low Impedance Regime

If the required inductance and available volume for each stage is in the single-turn regime (Fig. 4), both  $Q_L$  and  $v_r$  are impacted by the inductance  $L$ . This scenario arises if the desired resistances  $R_p$  or  $R_s$  are very low ( $\ll 1 \Omega$ ), or a large number of stages is to be used. In this case, dividing the total volume equally among different stages is not optimal since some stages may have higher-Q inductors than other stages and it may be more efficient to devote higher-Q stages for

larger voltage transformation and larger volumes for lower-Q inductors. Thus, the optimum volume and transformation ratio for each stage are no longer  $\mathcal{V}/n$  and  $v_r^{1/n}$  respectively and optimization is required.

The optimization result depends on whether the matching network is low-pass or high-pass, and the desired shunt-leg and series-leg resistances  $R_p$  and  $R_s$ . In this paper, we present an inductor design optimization for a high-pass matching network. To emphasize the maximum effect of (11) on the result, we choose  $R_s$  to be an extremely low  $0.1 \text{ m}\Omega$  for demonstration. The final results may be different for a higher  $R_s$  and converge to simple scaling of linear dimensions for  $R_s \gtrsim 0.1 \Omega$  in the range of volumes shown in Fig. 4. The  $0.1 \text{ m}\Omega$  resistance is chosen considering Fig. 4 and the 13.56 MHz operation frequency, and may not be useful for actual impedance transformation due to the very low impedance. However, for high power operation for which much larger inductor volumes than shown in Fig. 4 are available or required,  $R_s$  may not need to be as low for  $Q_L$  to be dependent on  $L$ . Moreover, for higher operation frequency ( $\gtrsim 100 \text{ MHz}$ ), the value of  $R_s$  for which this effect is triggered may be as high as  $1 \Omega$ .

We optimize the efficiency  $\eta$  of a 2-stage matching network assuming  $R_s = 0.1 \text{ m}\Omega$ . For fixed values of  $v_r$ , particle swarm optimization is performed to maximize the efficiency with respect to  $v_{ri}$  and  $\mathcal{V}_{Li}$  subject to the transformation ratio and volume constraints. The total volume is assumed to be  $1 \text{ cm}^3$ . Figs. 7 and 8 shows the optimization results. For  $v_r \lesssim 4.3$ , only one stage is responsible for the entire transformation and occupies all of the volume whereas the other stage performs no transformation and occupies no volume. This agrees with Fig. 6 that a single-stage network is the most efficient for  $v_r < 5.3$ . The difference in the optimal  $v_r$  breakpoint between the two cases is due to the difference in  $R_s$ . For larger  $v_r$ , the transformation ratio and the volume of the two stages are different and depend on  $v_r$ . The higher- $Z$  stage is in general responsible for a larger transformation ratio (for  $v_r \gtrsim 7.5$ ) and occupies a smaller volume ( $\approx 0.4 \text{ cm}^3$ ). This is because the lower- $Z$  stage is in general less efficient, and it is therefore more efficient to dedicate the higher- $Z$  stage for a larger portion of  $v_r$ . And a larger volume needs to be reserved for the less-efficient lower- $Z$  stage to maximize the overall efficiency.

### C. General Design Rules

We have discussed the optimization of matching network efficiency for the two cases of varying the inductor size and presented the results for  $v_r < 100$ . Power conversion applications usually require  $v_r < 20$ , and we present general matching network design rules for these applications.

Based on Figs. 5–7, it is most efficient to use a single-stage matching network for  $v_r \lesssim 5$  and a 2-stage network for  $5 \lesssim v_r \lesssim 20$ . The inequalities are only approximate because the optimum  $v_r$  breakpoints between different number of stages differ slightly depending on the required shunt-leg and series-leg impedances.



TABLE I  
MATCHING NETWORK OPTIMUM NUMBER OF STAGES AND TRANSFORMATION RATIOS

		1 stage	2 stages	3 stages
fixed-volume ( $\mathcal{V}_{tot} = 1 \text{ cm}^3$ )	$Q_{Li}$	200	159	139
	$v_{ropt}$	$1 < v_r < 5.3$	$5.3 < v_r < 18.6$	$19.2 < v_r < 63.0$
fixed-Q ( $Q_{Li} = 200$ )	$\mathcal{V}_{tot}$	$1 \text{ cm}^3$	$2 \text{ cm}^3$	$3 \text{ cm}^3$
	$v_{ropt}$	$1 < v_r < 3.0$	$3.0 < v_r < 6.9$	$6.9 < v_r < 15.6$

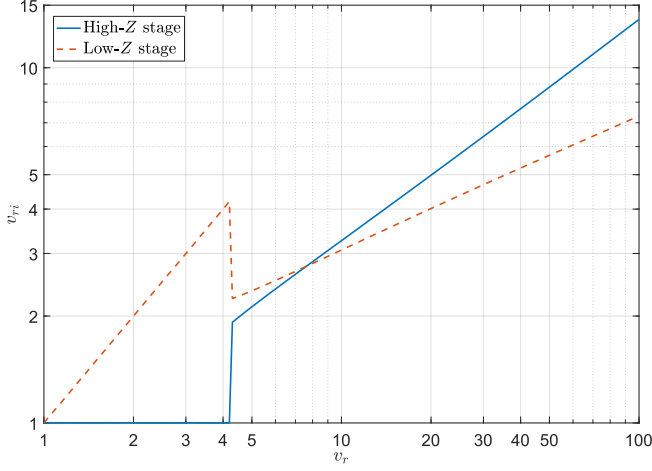


Fig. 7. Optimum transformation ratio for each stage  $v_{ri}$  vs. overall transformation ratio  $v_r$  of a 2-stage matching network for low-impedance transformation.

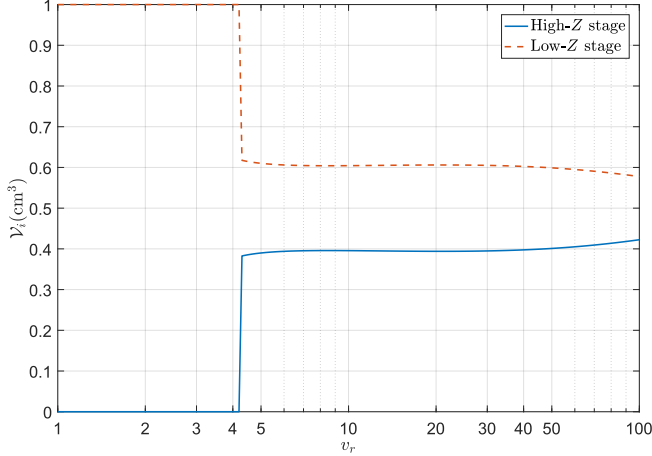


Fig. 8. Optimum volume for each stage  $\mathcal{V}_i$  vs. overall transformation ratio  $v_r$  of a 2-stage matching network for low-impedance transformation.

For a 2-stage network, if both of the required inductances are sufficiently large, it is most efficient to split the transformation and the volume equally between the two stages. The inductance is considered high if it is in the multi-turn regime, approximately defined based on the boundary in Fig. 4 as

$$L_i \gtrsim 10^{-6} \sqrt[3]{\mathcal{V}_{Li}}. \quad (12)$$

Although this limit is estimated from the blue dashed line in Fig. 4, which is specific for 13.56 MHz, the limit also applies for other operating frequencies. This is because the only frequency dependence of  $Q_L$  in (9) and (11) is via  $\delta$ , which impacts  $Q_L$  in both multi-turn and single-turn regimes equally. Thus, a difference in operating frequency will shift

the level of contour plot in Fig. 4 but will not change the position of the knee in the contour plot.

However, if the required inductances are much smaller than the limit in (12), the lower-impedance stage should occupy approximately 60% of the total volume while the higher-impedance stage fills the remaining 40%. The  $v_{ri}$  split in Fig. 7 gives the highest efficiency. However, the optimum  $v_{ri}$  for the two stages for  $5 \lesssim v_r \lesssim 20$  are not much different from each other. Thus, it may be simpler to split  $v_r$  equally and keep the 60-40 volume split while sacrificing slightly in the efficiency.

For higher  $v_r$ , the optimum number of stages can be chosen based on Fig. 4. As with 2-stage networks, the transformation ratio and the volume can be split equally among all the stages if all the required inductances are high enough. Otherwise,  $v_{ri}$  and  $\mathcal{V}_{Li}$  need to be optimized for the desired operating points.

The fixed-volume analysis of this paper and the fixed-Q analysis of [1] both assume that the input and load impedances of each stage of the matching network are purely resistive. This results in optimum number of stages that should be used for any desired transformation ratio  $v_r$ . However, only the input and load impedances of the overall matching network are limited by the applications, and the intermediate impedances between different stages can be complex. Allowing these intermediate impedances to be complex gives additional degrees of freedom in designing multistage matching networks. In the fixed-Q case, this results in a higher efficiency than discussed in [1], and the efficiency approaches an asymptotic limit as the number of stages increases [2]. Incorporating the fixed-volume analysis discussed in this paper to the complex-impedance optimization of [2] can give a better understanding on this asymptote and is a topic for future research.

The results in this paper were derived using specific values of  $f$  and  $R_s$ . The operating frequency is assumed to be 13.56 MHz throughout the paper. Because of the dependence of  $Q_L$  on  $f$ , the achievable matching network efficiency will be different if a different frequency is used; however, as discussed in Section IV-A, the optimum number of stages as a function of  $v_r$  remains approximately constant. The limit on the inductance values for the two different cases is also independent of operating frequency. Moreover, the results in Section IV-B were derived using  $R_s = 0.1 \text{ m}\Omega$  to demonstrate the effect of the inductor design optimization on the efficiency of the matching network, and may only apply for operation at very high power or frequency. For cases in which the inductance is only slightly smaller than the limit in (12), the matching network design needs to be optimized for the specific operating point required.

TABLE II  
MATCHING NETWORK DESIGN AND CHARACTERISTICS

	1 stage	2 stages	
		High-Z stage	Low-Z stage
$C_i$ (pF)	60.6	33.9	135.5
$L_i$ (μH)	2.42	5.42	1.36
$V_{Li}$ (cm <sup>3</sup> )	1	0.5	0.5
$N$	16	20	14
$r_L$ (mm)	6.0	5.9	4.6
$w_L$ (mm)	8.9	4.6	7.5
$Q_{L,theory}$	199	152	158
$\eta_{theory}$ (%)	96.15	95.60	
AWG	26	32	26
$L_{meas,1}$ (μH)	2.45	5.34	1.35
$L_{meas,2}$ (μH)	2.46	5.35	1.36
$Q_{L,meas,1}$	168	145	138
$Q_{L,meas,2}$	162	141	132
$\eta_{theory,Qmeas}$ (%)	95.36	95.10	
$\eta_{meas}$ (%)	95.36	94.92	

## V. EXPERIMENTAL VERIFICATION

We choose a voltage transformation ratio  $v_r$  of 4 (asterisks in Fig. 5) to experimentally verify the results of scaling of linear dimensions in Section IV-A. In the fixed- $Q$  analysis of [1], the efficiency of a 2-stage network (both with  $Q_L = 200$ ) is 98.27%, higher than that of a 1-stage network of 98.06%. However, when the total volume is constrained, a 2-stage network only has an efficiency of 97.83% since the inductor in each stage will only have  $Q_L = 159$ . Thus, we build 1- and 2-stage matching networks with 1 cm<sup>3</sup> total inductor volume to verify that a 1-stage network is more efficient than a 2-stage network for  $v_r = 4$  when the total volume is constrained.

### A. Design

High-pass L-section matching networks (inductor in the shunt-leg and capacitor in the series-leg) with 1 stage and 2 stages were designed to transform a series-leg impedance  $R_s$  of 50 Ω to a shunt-leg impedance  $R_p$  of 800 Ω at 13.56 MHz. For the 1-stage network,  $v_r = 4$  gives  $Q_t = \sqrt{15}$  and equating it to the shunt-leg quality factor  $Q_p = R_p/(\omega L)$  gives  $L = 2.42$  μH and the series-leg quality factor  $Q_s = 1/(\omega C R_s)$  gives  $C = 60.6$  pF. Repeating the same calculation for the 2-stage network, using  $v_{ri} = 2$  and  $Q_t = \sqrt{3}$  gives the required inductance and capacitance values for the lower-impedance transformation from 50 Ω to 200 Ω followed by the higher-impedance transformation from 200 Ω to 800 Ω. Table II gives the required passive component values for 1- and 2-stage networks with  $v_r = 4$  to transform 50 Ω to 800 Ω.

The required inductance values need to be achieved within 1 cm<sup>3</sup> for the 1-stage network and 0.5 cm<sup>3</sup> for the 2-stage network. The required solenoid radius  $r_L$  is calculated for various numbers of turns  $N$  to achieve the desired  $L$  (similar to Fig. 3), and the  $(N, r_L)$  pair that gives the highest  $Q_L$  is chosen for each inductor. Table II also gives the optimal

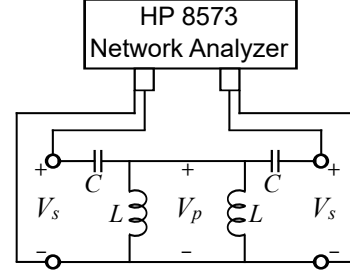


Fig. 9. Experimental setup for measuring matching network efficiency. Two identical matching networks are connected back-to-back to transform 50 Ω to 800 Ω and back to 50 Ω. The network efficiency is equivalent to the S21 power gain measured by the network analyzer.

inductor designs and  $Q_L$  as predicted by (9). The 2-stage low-Z inductor is approximately a smaller version of the 1-stage inductor, with all the dimensions and the resulting  $Q_L$  scaled by approximately  $1/\sqrt[3]{2}$ . On the other hand, the 2-stage high-Z inductor has similar  $r_L$  as the 1-stage inductor but half the  $w_L$ . This is not the optimal design for this particular inductor but the predicted  $Q_L$  of 152 is within 4% of the optimal  $Q_L$  158 which can be achieved by scaling all the dimensions equally.

### B. Experimental Setup

The wire gauges for the inductors were chosen such that all the turns fits into a single layer. The inductances and the corresponding quality factors were measured using an Agilent 4294A impedance analyzer and the results are in Table II. The measured quality factors are about 10–15% smaller than the predicted quality factor; the difference can be attributed to the effect of fringing fields on the inductor winding resistance, which is not included in (8). Low-loss capacitors (ATC 800B series) are used to achieve the required capacitance.

The efficiency of the matching networks was measured using a network analyzer. Two identical networks were built for both 1-stage and 2-stage networks in order to perform back-to-back transformation from 50 Ω to 800 Ω and back to 50 Ω (Fig. 9). The same back-to-back transformation setup is also used in [1] for measuring the efficiency of matching networks. This setup allows matching both end impedances to the 50 Ω output impedance of the network analyzer, which minimizes the reflected power and simplifies the extraction of efficiency from the measured S-parameters; the efficiency simply equals the S21 power gain. The lower efficiency of two back-to-back networks is also easier to measure than the higher efficiency of a single network.

### C. Results

The measured peak efficiencies  $\eta_{meas}$ , as well as the efficiencies predicted using theoretical inductor quality factors ( $\eta_{theory}$ ) and measured inductor quality factors ( $\eta_{theory,Qmeas}$ ) are included in Table II. The close match between  $\eta_{meas}$  and  $\eta_{theory,Qmeas}$  validates the efficiency analysis. Even though the measured and predicted  $Q_L$  are about 10–20% different, the scaling in (6) is approximately true.

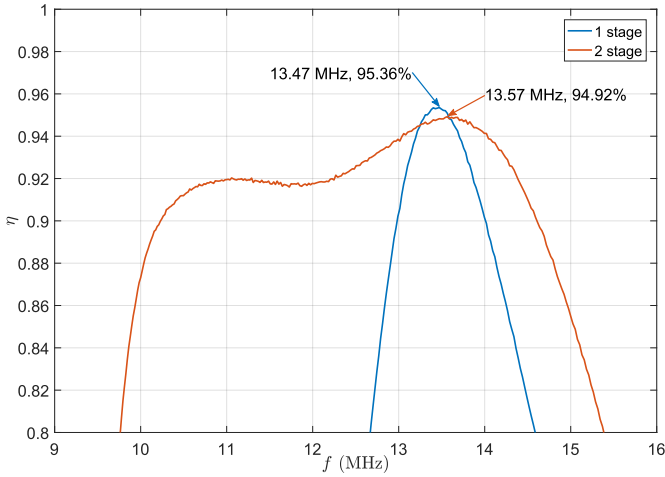


Fig. 10. Measured efficiency vs. frequency for back-to-back pairs of 1- and 2-stage matching networks described in Table II, with corresponding maximum efficiency points.

Thus, the relative efficiencies of 1-, 2- and 3-stage networks in Fig. 5 are still valid, and it is verified by  $\eta_{theory, Q_{meas}}$ .

This relation is also confirmed by the measured efficiencies of back-to-back 1-stage and 2-stage networks as shown in Fig. 10. The 1-stage networks back-to-back have a peak efficiency of 95.36% (each network efficiency  $\approx 97.65\%$ ) at 13.47 MHz and the 2-stage networks back-to-back 94.92% (each network efficiency  $\approx 97.43\%$ ) at 13.57 MHz. The networks can be fine-tuned so that the peak efficiencies occur at the desired 13.56 MHz. However, the figure shows that the 1-stage network is indeed more efficient than the 2-stage network of the same volume for  $v_r = 4$ .

This experimental result verifies the model of scaling the linear dimensions and the effect of such scaling on the efficiency of a single-stage and multistage matching network shown in Figs. 5 and 6. As a result, the fixed-volume analysis presented in this paper provides a better perspective on the optimum number of stages that should be used for various transformation ratios whereas the fixed-Q analysis in [1] provides an upper bound on the number of stages that should be considered when designing matching networks. Because adding an extra stage to a matching network creates additional challenges regarding design, tuning, parasitics and termination, there is an inherent implementation advantage to using fewer stages in a matching network. The analysis in this paper provides verified results on the number of stages that need to be used to obtain the highest possible efficiency for the desired voltage transformation ratio.

## VI. CONCLUSION

We have presented two scaling models to describe the variation of inductor performance with size and used them to analyze the efficiency of matching networks. A simple scaling of inductor linear dimensions can be used if the required inductance is sufficiently high; in such cases, an equal split of the volume and voltage transformation ratios among all the stages is the most efficient. The optimum number of stages derived in this case was experimentally verified by building 1-

and 2-stage matching networks using well-designed inductors in a total volume of  $1 \text{ cm}^3$ . The resulting inductor quality factors scales similarly to the linear scaling model, and the measured efficiencies of the matching networks closely match the efficiencies predicted using the measured quality factors.

For low-impedance transformation which requires very low inductances, the inductor design needs to be optimized for the required inductance and available volume, resulting in an uneven split of the volume and the voltage transformation ratios among the stages.

Simple design rules for matching networks with transformation ratios lower than 20 were also presented to address a wide range of power conversion applications. Although some results are specific to particular frequencies and impedances, the design rules in general can be applied for most cases.

Because adding extra stages to a matching network usually involves complications regarding implementation, fewer stages are in general preferable to a larger number of stages. The fixed-Q analysis of multistage matching networks [1] provides an upper bound on the number of stages that need to be considered when designing matching networks. By combining that analysis with scaling models of inductor performance, this paper provides a basis for optimizing the efficiency of multistage matching networks within a constrained volume and calculating the optimum number of stages. This paper, however, assumed that the input and load impedances of each stage are purely resistive; relaxing that assumption may lead to different optimal efficiencies and design rules, and is a promising avenue for future research.

## ACKNOWLEDGMENT

This material is based upon work supported by the National Science Foundation under Grant Nos. 1507773 and 1610719.

## REFERENCES

- [1] Y. Han and D. J. Perreault, "Analysis and design of high efficiency matching networks," *IEEE Transactions on Power Electronics*, vol. 21, no. 5, pp. 1484–1491, 2006.
- [2] A. Kumar, S. Sinha, A. Sepahvand, and K. Afridi, "Improved design optimization for high-efficiency matching networks," *IEEE Transactions on Power Electronics*, 2017.
- [3] C. R. Sullivan, B. A. Reese, A. L. F. Stein, and P. A. Kyaw, "On size and magnetics: Why small efficient power inductors are rare," in *3D Power Electronics Integration and Manufacturing (3D-PEIM), International Symposium on*. IEEE, 2016, pp. 1–23.
- [4] J. T. Strydom and J. D. van Wyk, "Volumetric limits of planar integrated resonant transformers: a 1 MHz case study," *IEEE Transactions on Power Electronics*, vol. 18, no. 1, pp. 236–247, 2003.
- [5] J. A. Ferreira and J. D. van Wyk, "Electromagnetic energy propagation in power electronic converter: toward future electromagnetic integration," *Proceedings of the IEEE*, vol. 89, no. 6, pp. 876–889, 2001.
- [6] E. Waffenschmidt and J. Ferreira, "Embedded passive integrated circuit for power converters," in *33rd Annual IEEE Power Electronics Specialists Conference (PESC)*, vol. 1, 2002, pp. 12–17.
- [7] P. A. Kyaw and C. R. Sullivan, "Fundamental examination of multiple potential passive component technologies for future power electronics," in *IEEE 16th Workshop on Control and Modeling for Power Electronics (COMPEL)*, 2015.
- [8] "Radio instruments and measurements," *Bureau of Standards Circular*, vol. C74, p. 252, January 1937.